

Supporting Information for:
**Study of the Elusive Hydration of Pb^{2+} from the
Gas Phase to the Liquid Aqueous Solution:
Modeling the Hemidirected Solvation with a
Polarizable MCDHO Force-Field**

C. I. León-Pimentel,* M. Martínez-Jiménez, and H. Saint-Martin

*Instituto de Ciencias Físicas, Universidad Nacional Autónoma de México, Apdo. Postal
48-3, Cuernavaca, Morelos 62251, México.*

E-mail: clp@icf.unam.mx, bennykun@gmail.com

Phone: +52 1 777 104 55 63

The MCDHO2.1 water model

Though the MCDHO2 water model¹ already rendered most of the experimental data used to test water models, it still had two main drawbacks: on one hand, it yielded a somewhat low density, and on the other, it kept a nonzero coefficient for a dispersion term in the OH interaction. The new parametrization MCDHO2.1 was aimed at overcoming these drawbacks, without lowering the general performance in simulations of the condensed phases.

The analytical potential includes intramolecular interactions, thus each water molecule has an individual energy

$$\begin{aligned}
 U_m = & \frac{1}{2}kr_O^2 + \frac{Z_H^2}{R_{1,2}} + \sum_{\beta=1}^2 \left\{ \frac{qZ_H}{r_\beta} \left[1 - \left(\frac{r_\beta}{\lambda} + 1 \right) \exp \left(-2\frac{r_\beta}{\lambda} \right) \right] + \frac{Z_O Z_H}{R_\beta} \right. \\
 & + D \{ \exp [-2\gamma (R_\beta - r_{eq})] - 2 \exp [-\gamma (R_\beta - r_{eq})] \} \\
 & \left. + a_1(\theta - \theta_e) + a_2(\theta - \theta_e)^2 + a_3(\theta - \theta_e)^3 + a_4(\theta - \theta_e)^4 \right\} \quad (1)
 \end{aligned}$$

and the total energy of a system with N molecules is thus

$$\begin{aligned}
 U_{total} = & \sum_{n=1}^N \sum_{m=1}^{n-1} \left\{ \left(\frac{A}{r_{nm}} \right) - \left(\frac{B}{r_{nm}} \right)^2 + \frac{q^2}{r_{nm}} \right. \\
 & + \sum_{\beta \in m} \frac{qZ_\beta}{r_{n\beta}} \left[1 - \left(\frac{r_{n\beta}}{\lambda'} + 1 \right) \exp \left(-2\frac{r_{n\beta}}{\lambda'} \right) \right] \\
 & \left. + \sum_{\alpha \in n} \sum_{\beta \in m} \left[\left(\frac{A_{\alpha\beta}}{r_{nm}} \right) - \left(\frac{B_{\alpha\beta}}{r_{nm}} \right)^2 + \frac{Z_\alpha Z_\beta}{R_{\alpha\beta}} \right] \right\} \quad (2)
 \end{aligned}$$

The new set of parameters is shown in table 1 along with the previous set.

The MD simulations of liquid water used the leap-frog scheme for the integration of the equations of motion, with $N_{int} = 1 \times 10^8$ steps and $\Delta t = 0.2$ fs. Simulations were performed under a NpT ensemble. Thermal coupling was implemented with the velocity rescaling method ($\tau_T = 0.1$) and the barostat with the isotropic Berendsen method ($\tau_P = 0.7193$).

Electrostatic interactions were calculated with the Ewald sum method (PME version).^{2,3} Periodic boundary conditions were used for the cubic simulation box whose original size was equal to 10^3 \AA^3 .

Table 1: Parameters of the MCDHO, MCDHO2 and MCDHO2.1 models. Detailed information in references.^{1,4}

Electrostatics	Z_H	Z_O	q_M	k_M	λ_M
MCDHO	0.62	2.66	-3.90	1.48	1.90
MCDHO2 and MCDHO2.1	0.62	2.00	-3.94	1.00	1.90
$r(O-H)$	D_{OH}	r_{OH}^{eq}	γ_{OH}		
MCDHO	0.544688	1.2044644	1.1677636		
MCDHO2 and MCDHO2.1	0.42954902	1.3440633	1.1131102		
$\angle HOH$	θ_{HOH}^{eq}	a_{HOH}	b_{HOH}	c_{HOH}	d_{HOH}
MCDHO	1.875	0.027018	0.045926	-0.018199	-0.00942
MCDHO2 and MCDHO2.1	1.927	0.031621	0.043914	-0.012721	-0.00866
intermolecular	λ'_M	A_{MM}	B_{MM}	B_{OH}	A_{HH}
MCDHO	1.1101	3.204243	2.027671	1.194170	2.442124
MCDHO2	1.1600	3.228656	1.962046	1.037891	
MCDHO2.1	1.1600	3.112274	1.934902		

Values are given in Hartree atomic units.

Only non-zero values are presented.

Equation of state ρ vs. T at $p = 1$ bar

Table 2 shows the numerical values of the density at $p = 1$ bar. The data set obtained by the numerical simulations was adjusted to the following analytical expression:

$$\rho = a + \frac{b}{T} + \frac{c}{T^2} + \frac{d}{T^3} + \frac{e}{T^4} + \frac{f}{T^5} \quad (3)$$

Table 2: Water density in the interval between 220 K and 360 K

MCDHO2.1			Experimental	
Temp. (K)	ρ (kg/m ³)	Error	Temp. (K)	ρ (kg/m ³)
220	979.736	1.8	222.5	940.0
240	982.86	0.65	250	991.3
260	994.647	0.12	260	997.0
270	998.443	0.09	270	999.5
280	1000.22	0.061	280	999.9
290	999.966	0.046	290	998.8
300	997.981	0.02	300	996.55
320	990.184	0.022	320	989.43
340	978.339	0.045	340	979.5
360	963.33	0.036	360	967.4

The fitted coefficient values are:

$$\begin{aligned}
 a &= -3996.21 & d &= 1.1423 \times 10^{12} \\
 b &= 6.7260 \times 10^6 & e &= -1.74 \times 10^{14} \\
 c &= -3.8378 \times 10^9 & f &= 1.0662 \times 10^{16}
 \end{aligned}
 \tag{4}$$

These are the data used for Fig. S1.

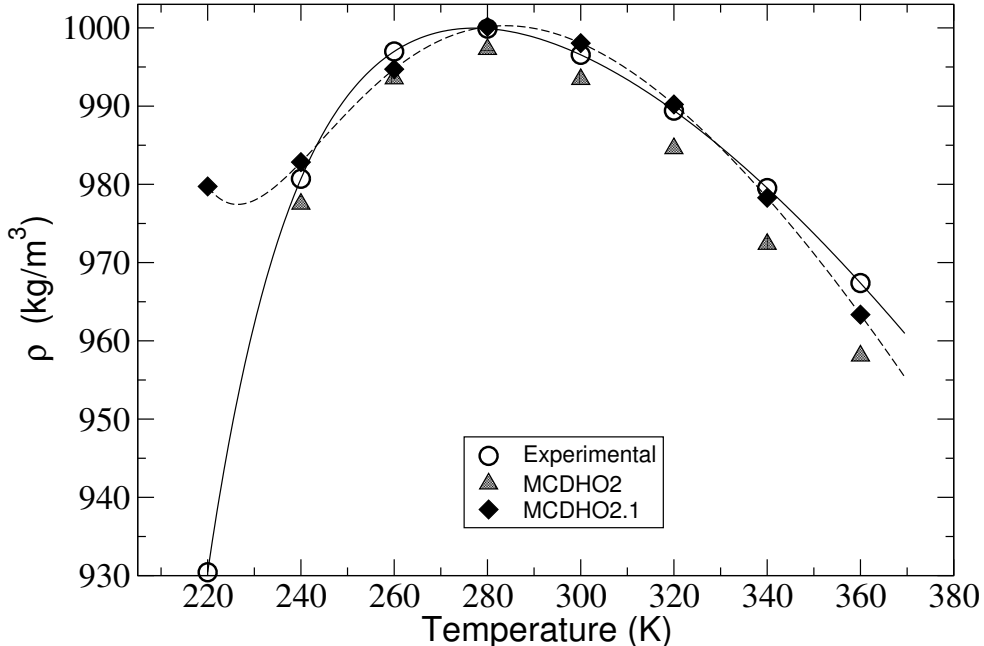


Figure S1: Comparison of the density ρ vs temperature T curve resulting from simulations with the MCDHO2.1 model to the previous MCDHO2 version and to experimental data.

Simulations of gas-phase $[\text{Pb}(\text{H}_2\text{O})_n]^{2+}$ clusters at $T = 300 \text{ K}$

The capability of the MCDHO model to mimic the behavior of the BOMD simulations of 4+2, 6+0 Holo, 6+0 Hemi, 4+4 and 8+0 clusters (see Fig. 1 of main text) is discussed here and compared to the results found with the sFF.

4+2 cluster

The Pb-O distances RDFs and ADFs found in the simulations of $[\text{Pb}(\text{H}_2\text{O})_6]^{2+}$ 4+2 cluster are shown in Figs. S1, S2 and S3, respectively. In agreement with the BOMD simulation, the MCDHO model retains two water molecules in the second shell for at least 13 ps, while the sFF coordinates the six water molecules to the ion. It can be seen from the RDFs that both the MCDHO and the sFF have wider Pb-O distance distributions than the BOMD. The ADFs of the sFF has major contributions from values around 900 and around 1700 which are indicative of a octahedral coordination very similar to the one found¹⁰ for microhydrated Mg^{2+} ; while the MCDHO present a pattern more similar to the one found with BOMD.

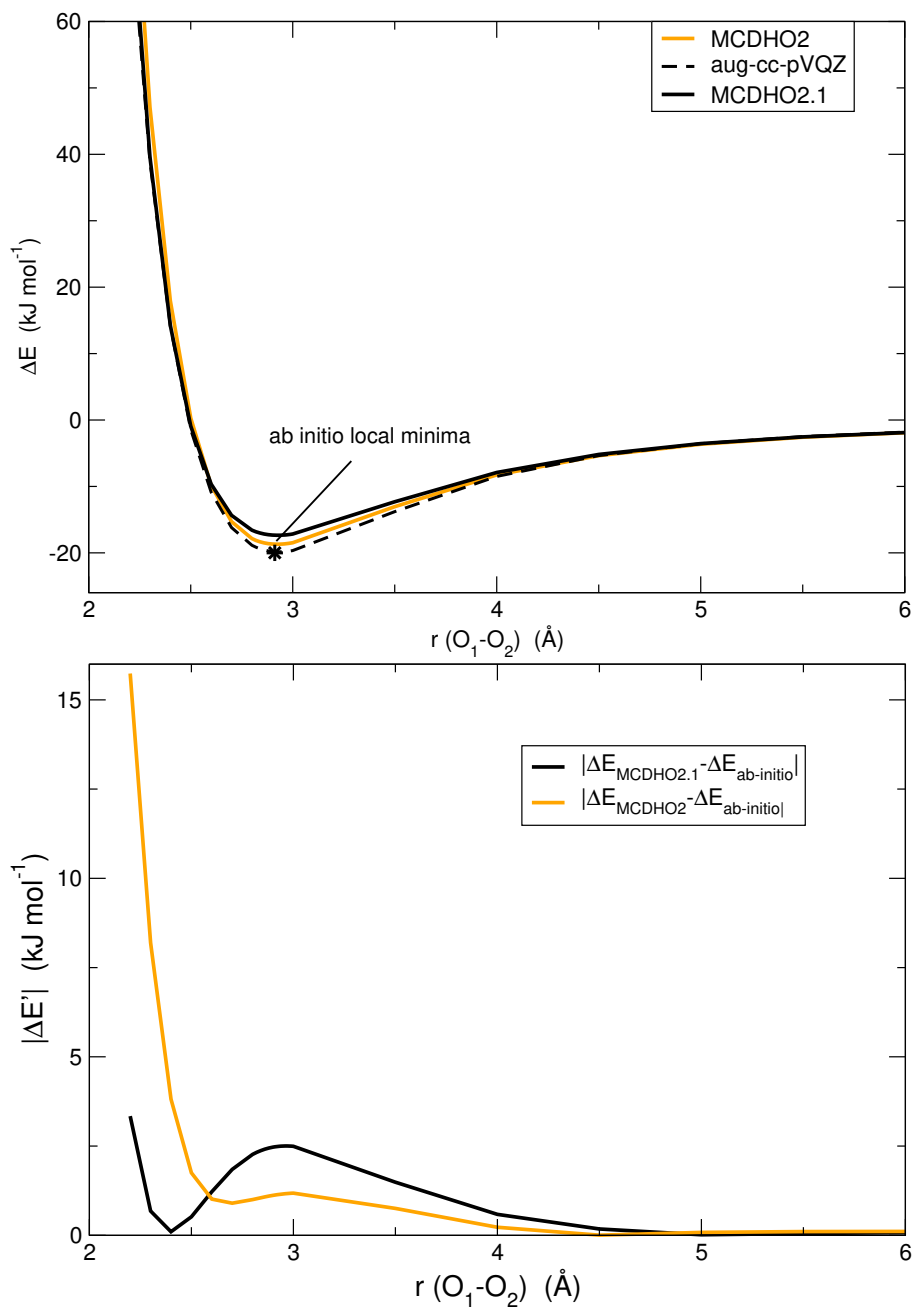


Figure S2: (Top) Comparison of the binding energy E_b of the water dimer as a function of the $r(\text{O} - \text{O})$ distance along the hydrogen-bonded configuration, with the MCDHO2.1 model to the previous MCDHO2 version and to high-quality *ab initio* calculations (MP2/aug-cc-pVQZ). (Bottom) Absolute values of the differences relative to high-quality *ab initio* calculations of the MCDHO2.1 and MCDHO2 models.

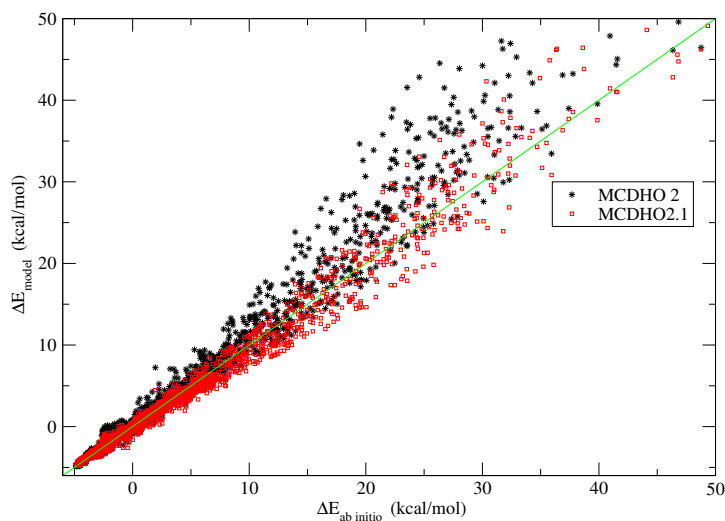


Figure S3: Comparison of the MCDHO2 and MCDHO2.1 water models to a reference PIES computed with SAPT.⁵

Table 3: Binding energies (kcal/mol) obtained for different water clusters with the MCDHO2 and MCDHO2.1 compared to the complete MP2/CBSL reported in Refs. ? ? ?

(H ₂ O) ₆ clusters			
	CBSL	MCDHO2	MCDHO2.1
Cage	-45.89	-42.40	-42.32
Prism	-45.87	-42.64	-42.71
Book	-45.60	-42.07	-41.93
Ring	-44.86	-41.11	-40.84
(H ₂ O) ₈ clusters			
D2D	-72.7	-67.29	-67.01
S4	-72.7	-67.29	-67.00
(H ₂ O) ₂₀ clusters			
Dodecahedron	-200.1	-185.92	-183.85
Fused cubes	-212.1	-198.55	-198.01
Face sharing	-215.2	-198.35	-197.23
Edge sharing	-217.1	-199.91	-198.80

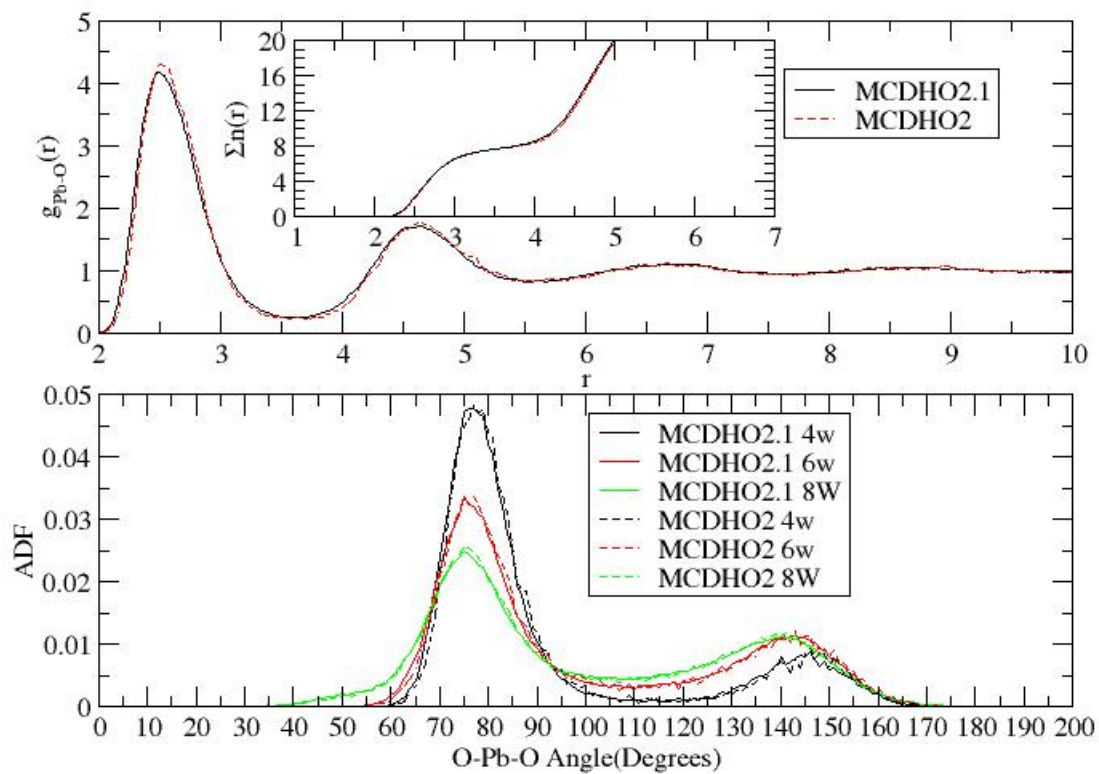


Figure S4: Comparison of the RDF's, cumulative coordination numbers and the ADF's obtained with MCDHO2 and MCDHO2.1 water model in the simulation of one Pb^{2+} ion in solution.

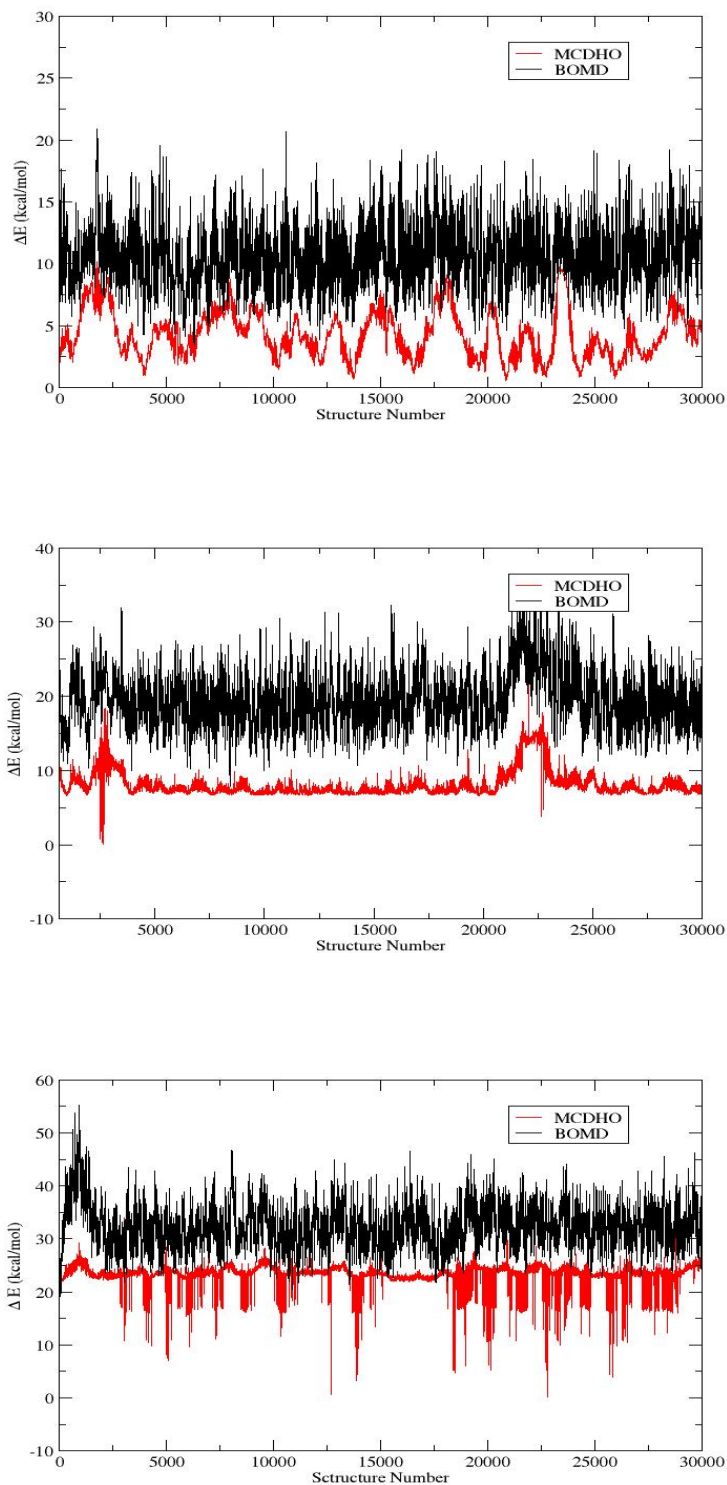


Figure S5: Comparison of ΔE (Energy of current structure minus energy of the lowest structure) from our model and from BOMD simulations. The structures were taken from the BOMD simulations of the (top) 4+0 cluster, (middle) 4+2 cluster and (bottom) the 4+4 cluster.

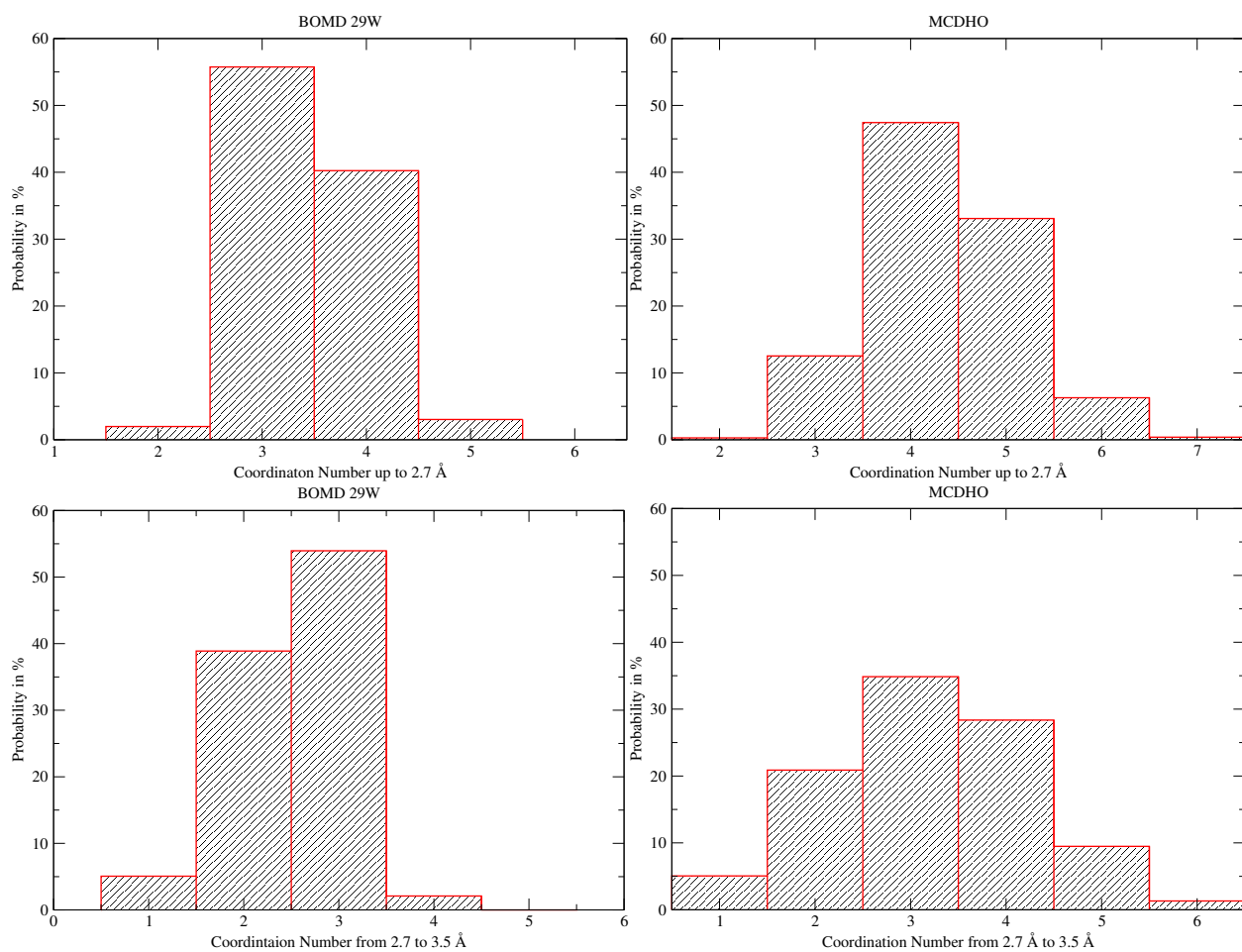


Figure S6: Mean coordination number of water molecules present in the BOMD (29w) and MCDHO simulations in the region 0 to 2.7 Å and 2.7 to 3.5 Å.

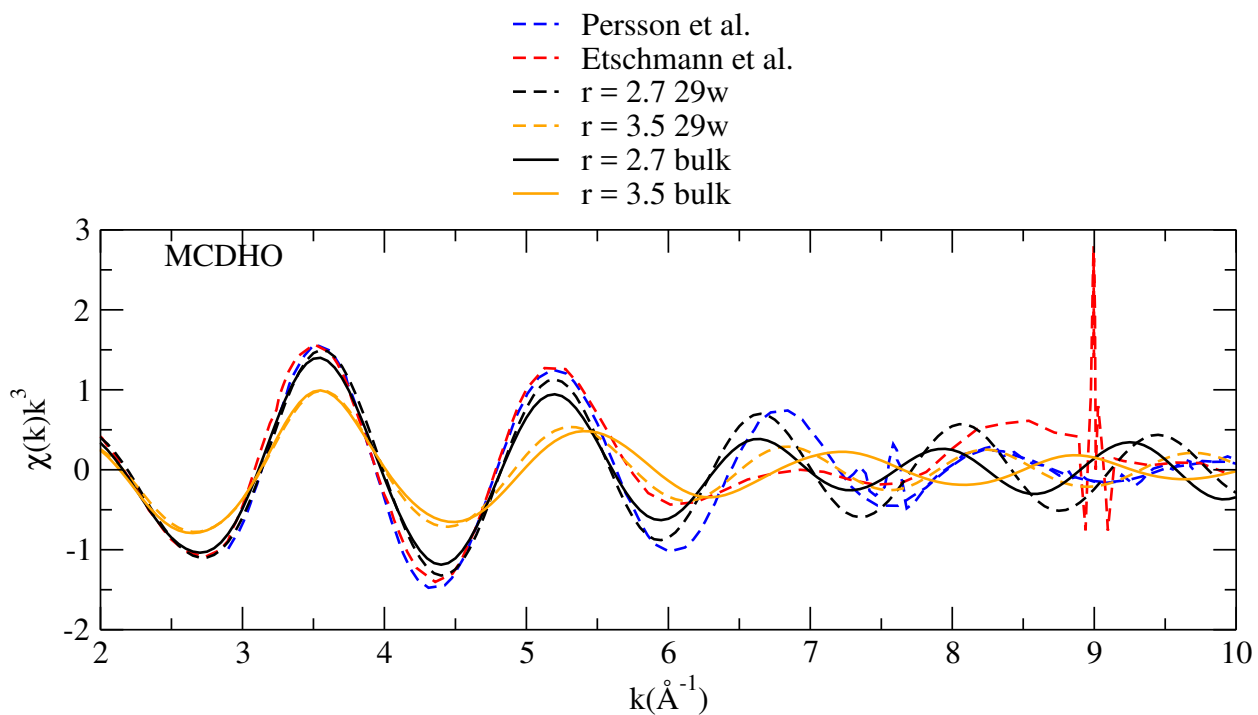


Figure S7: Calculated EXAFS spectra from: the MCDHO simulation of the 29w cluster (black and orange dashed lines) and the MCDHO simulation of the aqueous solution (black and orange lines). The blue and red dashed lines are the experimental spectra of Persson et al.⁶ and Etschmann et al.,⁷ respectively

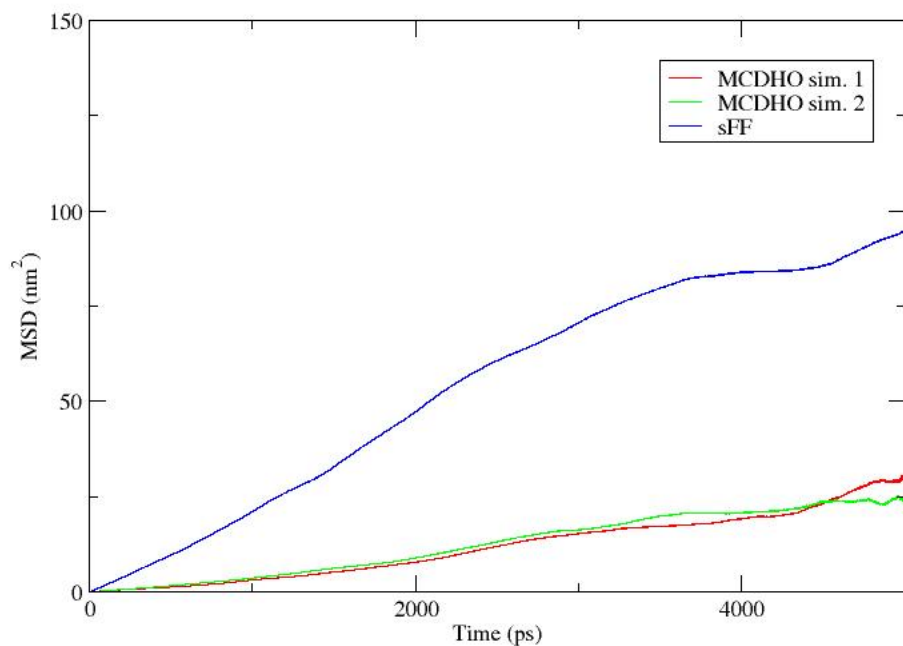


Figure S8: Mean Square Displacement plots of the Pb^{2+} ion for the classical MD simulations employing the sFF of ref. 8 and our MCDHO model. The results of two simulations are shown for the latter. The diffusion coefficients were computed using the utilities in the GROMACS⁹ software package, that produce an estimate of the standard errors in the range of $0.01 \times 10^{-5} \text{ cm}^2/\text{s}$; however, it is a better practice to use a block average scheme that shows the precision to reach only $0.1 \times 10^{-5} \text{ cm}^2/\text{s}$.

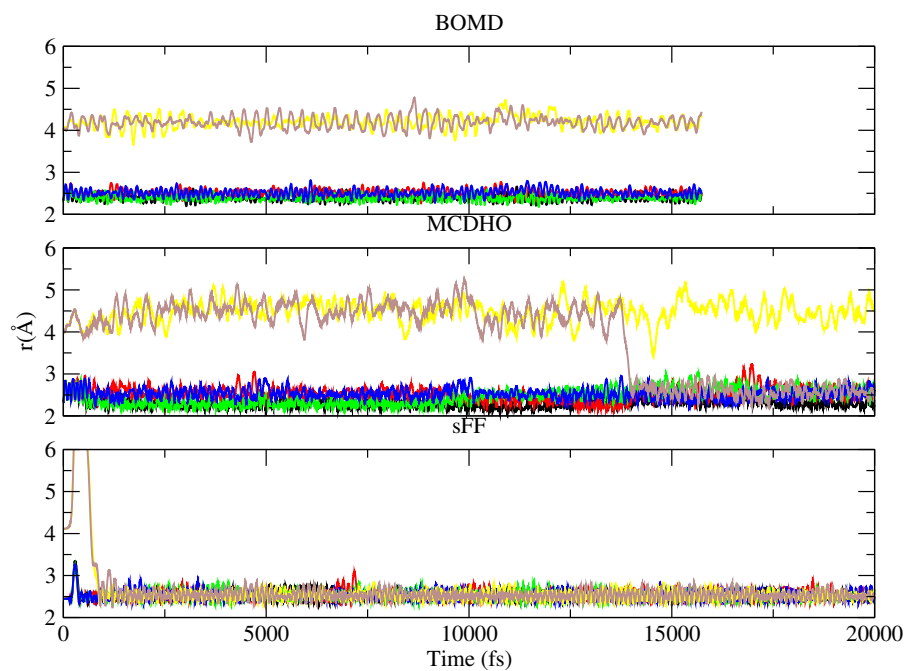


Figure S9: Pb-O distances found in the simulations of the 4+2 cluster (see Fig. 1 of main text) by means of: BOMD simulation (top), classical MD with MCDHO (middle), and classical MD with the sFF of de Araujo et al.⁸ (bottom). Only the first 20 ps are shown.

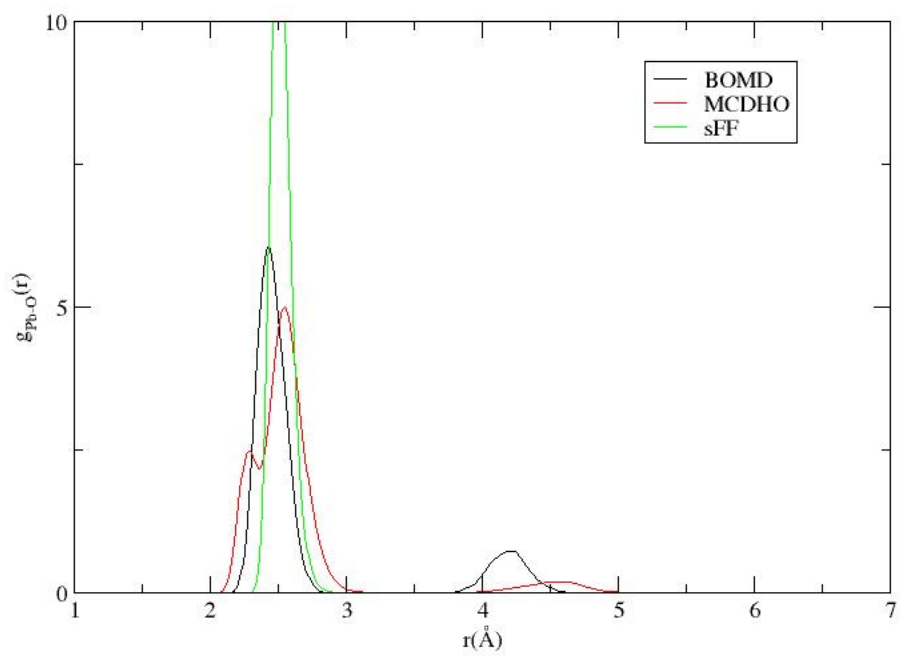


Figure S10: RDF's of the simulations of the 4+2 cluster (see fig. 3 of main text) employing: BOMD, classical MD with MCDHO, and classical MD with the sFF of de Araujo et al.⁸

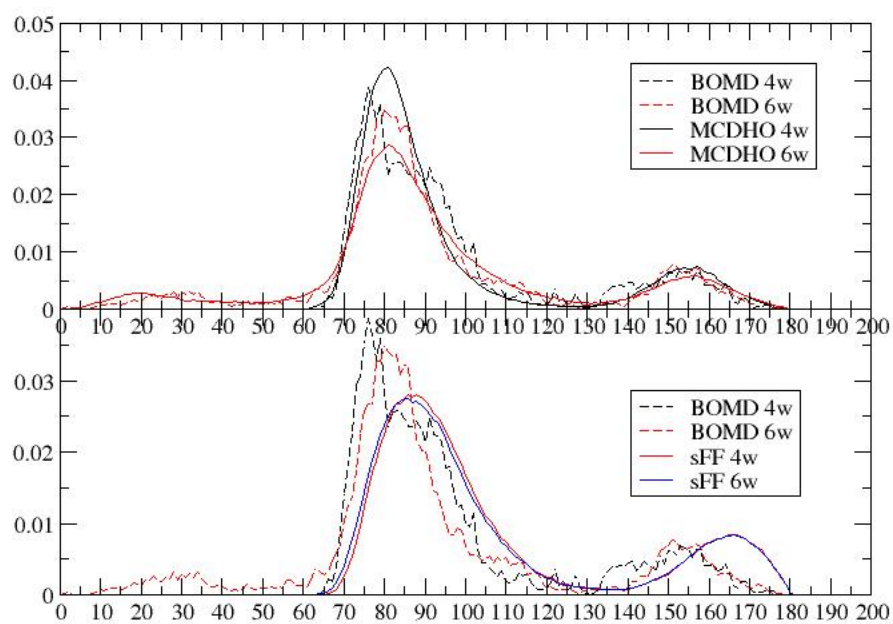


Figure S11: ADF's of the simulations of the 4+2 cluster (see Fig. 1 of main text) employing: BOMD, classical MD with MCDHO, and classical MD with the sFF of de Araujo et al.⁸

6+0 Holo cluster

As can be seen from figure S12, the BOMD simulation that started from this cluster evolved in a configuration of the type 4+2, neither MCDHO nor the sFF replicate this feature; hence, the models did not reproduce the ADF (see Fig. S14) of the BOMD simulation. Although, both models have a CN = 6, MCDHO produced a wider Pb-O distribution as shown by the RDF in Fig. S13 than the sFF. Also, it can be seen that the ADF of the sFF has more contributions from angles around 90° and near 170° than the MCDHO model, which has more contributions from angles around 80° and 150° , this is a signal of a more well oriented hydration shell in the sFF.

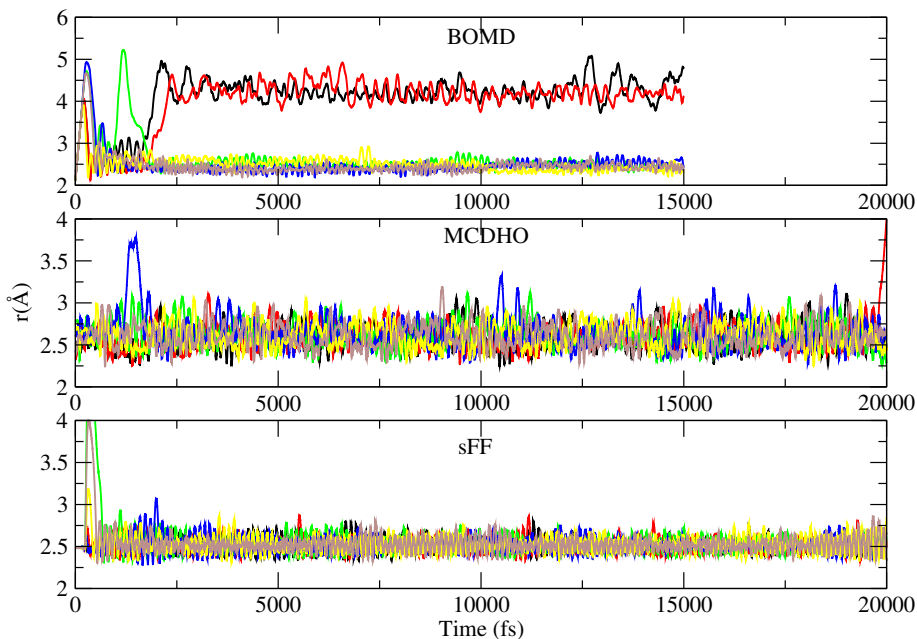


Figure S12: Pb-O distances found in the simulations of the 6+0 Holo cluster (see fig. 1 of main text) by means of: BOMD simulation (top), classical MD with MCDHO (middle), and classical MD with the sFF of de Araujo et al.⁸ (bottom). Only the first 20 ps are shown.

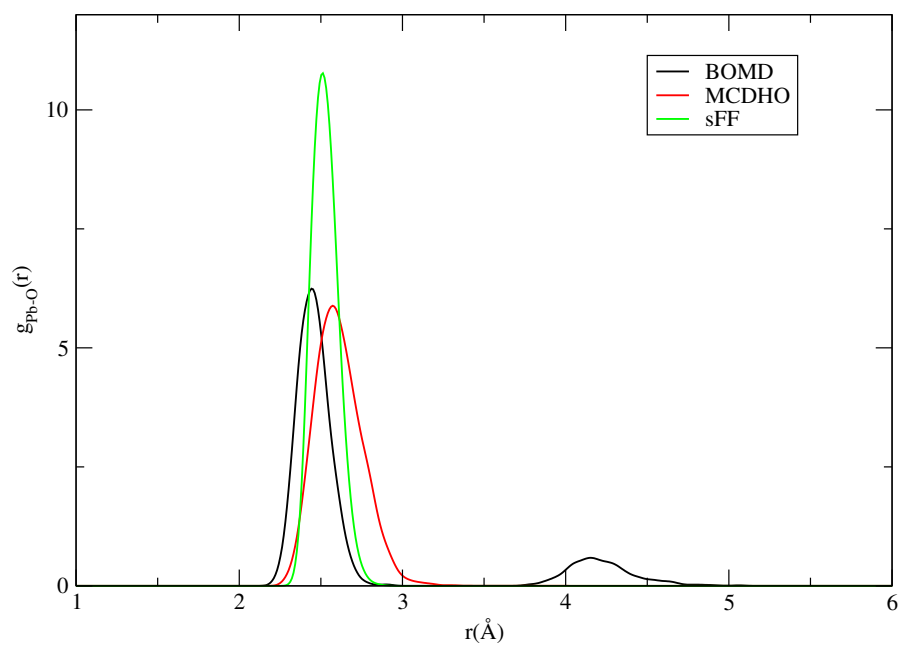


Figure S13: RDF's of the simulations of the 6+0 Holo cluster (see fig. 3 of main text) employing: BOMD simulation, classical MD with MCDHO and classical MD with the sFF of de Araujo et al.⁸

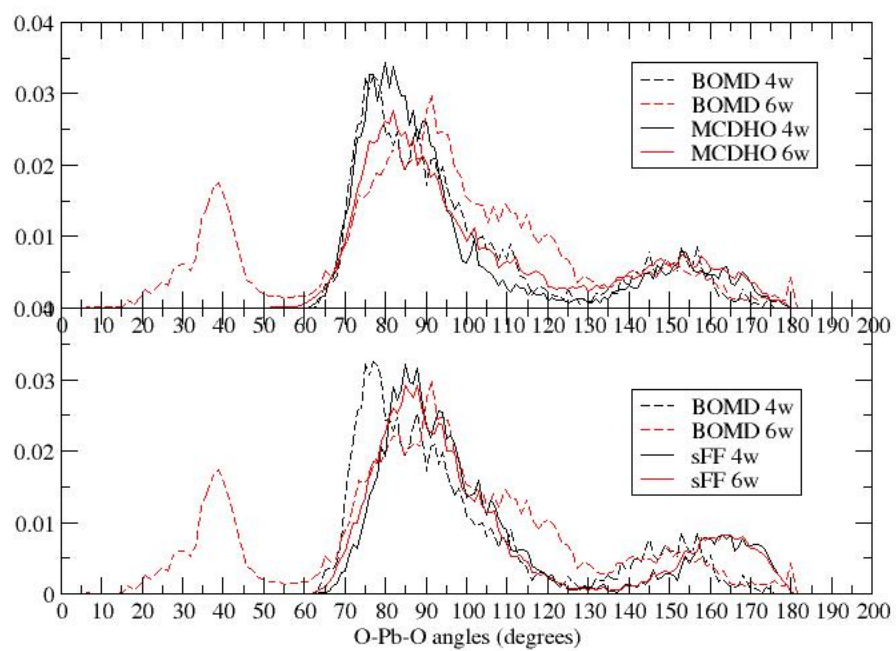


Figure S14: ADF's of the simulations of the 6+0 Holo cluster (see fig. 1 of main text) employing: BOMD simulation, classical MD with MCDHO and classical MD with the sFF of de Araujo et al.⁸

6+0 Hemi cluster

The BOMD simulation did not retain the initial coordination pattern and, similarly to what happened with the 6+0 holo simulation, changed to a 4+2 coordination pattern (see Fig. S15). Thus, neither the MCDHO model nor the sFF has similarities with the geometric motifs found in the BOMD simulation. However, it is interesting to note that the MCDHO produces a wider distribution of Pb-O distances (see Figs. S15 and S16) than the sFF and that the ADF varies considerably when taking 4 or 6 water molecules into account, this reflects that the dynamics observed in the 6+0 Holo and Hemi simulations differ with the MCDHO model.

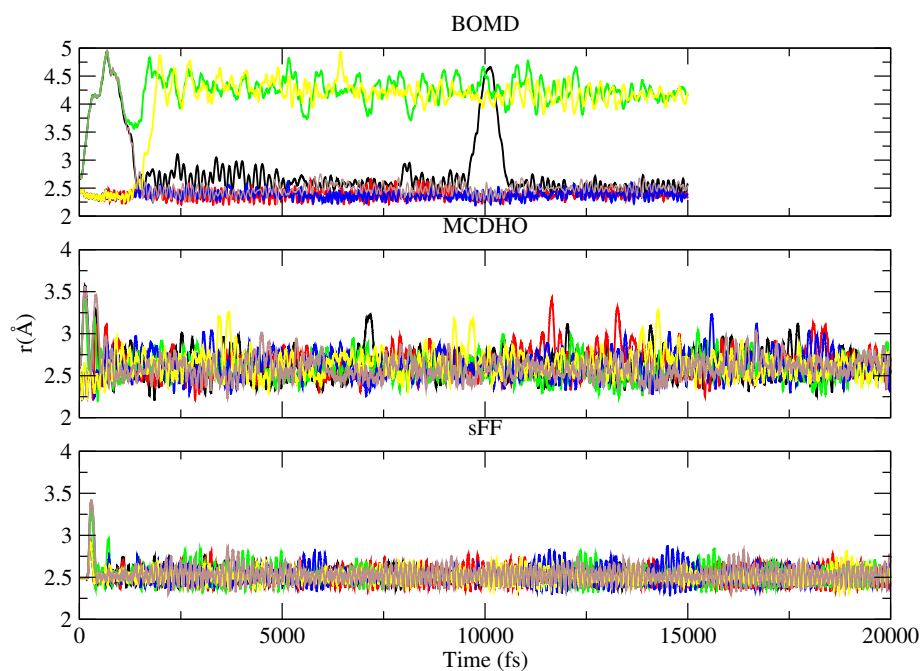


Figure S15: Pb-O distances found in the simulations of the 6+0 Hemi cluster (see fig. 1 of main text) by means of: BOMD simulation (top), classical MD with MCDHO (middle) and classical MD with the sFF of de Araujo et al.⁸ (bottom). Only the first 20 ps are shown.

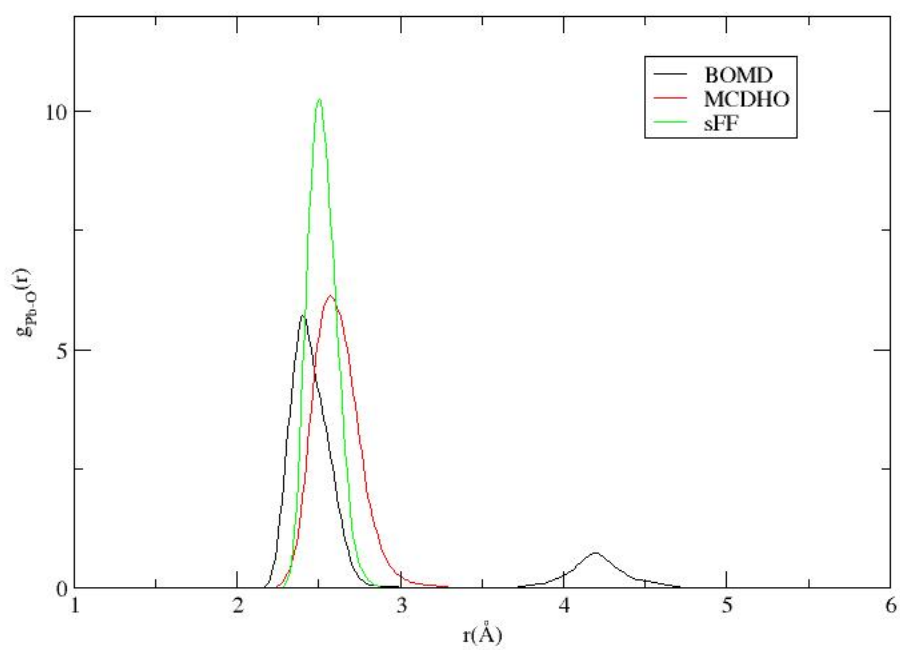


Figure S16: RDF's of the simulations of the 6+0 Hemi cluster (see fig. 1 of main text) employing: BOMD simulation, classical MD with MCDHO and classical MD with the sFF of de Araujo et al.⁸

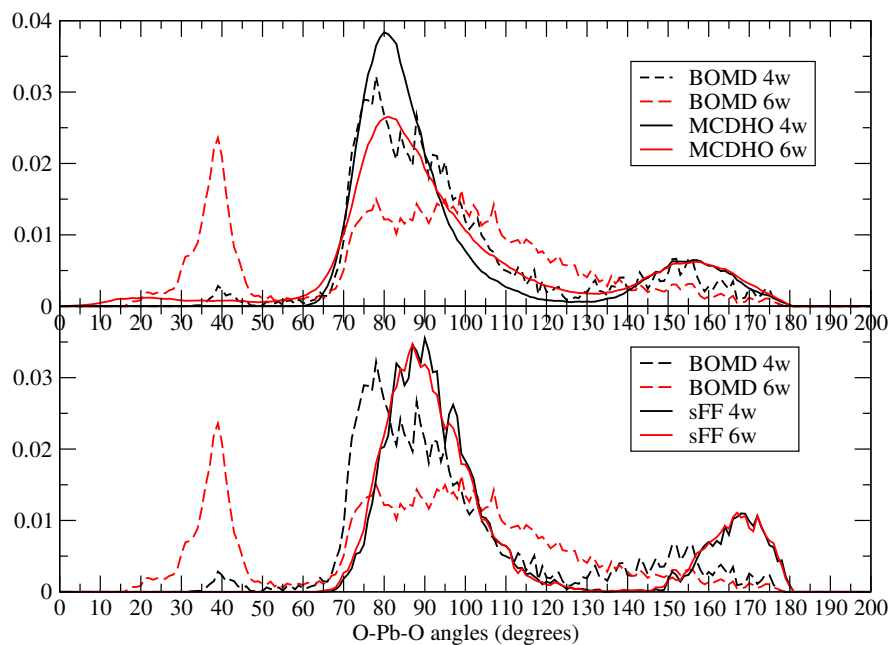


Figure S17: ADF's of the simulations of the 6+0 Hemi cluster (see fig. 3 of main text) employing: BOMD simulation, classical MD with MCDHO and classical MD with the sFF of de Araujo et al.⁸

4+4 cluster

The 4+4 cluster has a very symmetric configuration which is hard to retain by an empirical model when accounting for thermal motion. Neither the MCDHO nor the sFF were able to retain the 4+4 coordination. The MCDHO oscillated between a 5+3 and a 6+2 coordination, while the sFF yielded a 7+1 coordination (see Fig. S18). As depicted in Fig. S19, the RDFs of both models differ from that of BOMD, however the ADF with the 4 nearest water molecules in the MCDHO simulation turned out similar to that from BOMD (see Fig. S20), suggesting that the geometry of these 4 water molecules resembles the closest 4 in the BOMD simulation. In the other hand, the sFF did not show significant changes in the ADF when considering the 4, 6 or 7 closest water molecules, denoting a symmetrical coordination shell.

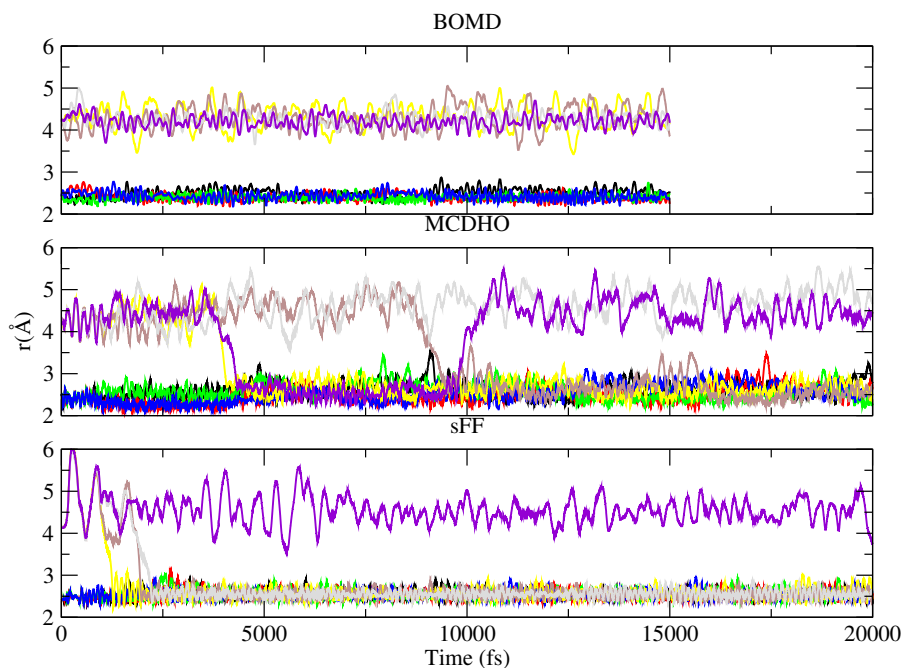


Figure S18: Pb-O distances found in the simulations of the 4+4 cluster (see fig. 1 of main text) by means of: BOMD simulation (top), classical MD with MCDHO (middle) and classical MD with the sFF of de Araujo et al.⁸ (bottom). Only the first 20 ps are shown.

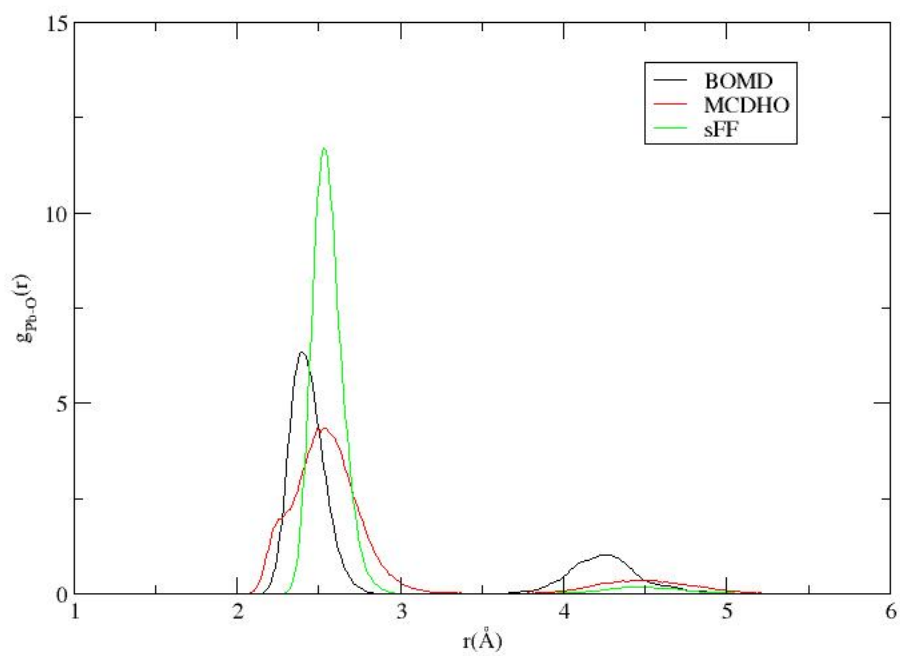


Figure S19: RDF's of the simulations of the 4+4 cluster (see fig. 3 of main text) employing: BOMD simulation, classical MD with MCDHO and classical MD with the sFF of de Araujo et al.⁸

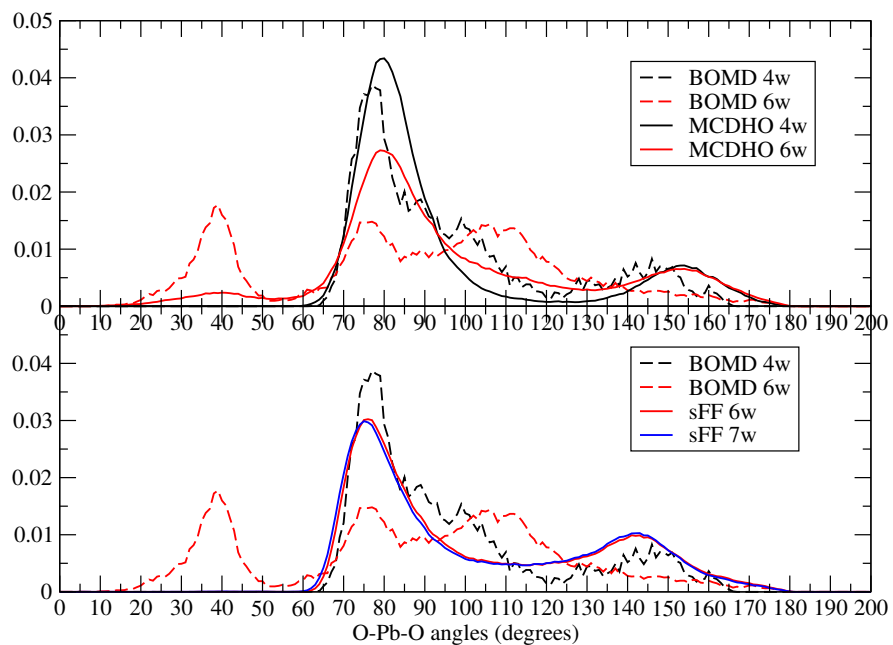


Figure S20: ADF's of the simulations of the 4+4 cluster (see fig. 1 of main text) employing: BOMD simulation, classical MD with MCDHO and classical MD with the sFF of de Araujo et al.⁸

8+0 cluster

The results of the $[\text{Pb}(\text{H}_2\text{O})_8]^{2+}$ 8+0 cluster simulations are shown in Figs. S21,S22 and S23. As this cluster is not the lowest energy isomer, none of the simulations was able to retain this configuration when the temperature comes into play. The BOMD simulation adopted a 6+2 and a 5+3+1 configuration for most of the simulation. The MCDHO showed a 6+2 configuration for more than 10 ps, while the sFF yielded a 7+1 configuration most of the time. Thus the similarities found in the ADFs are rather fortuitous, but again there is no significant difference in the ADF of the sFF when taking into account 4, 6 or 7 water molecules in the calculation, while a significant difference is found with MCDHO when taking 4 or 6 water molecules.

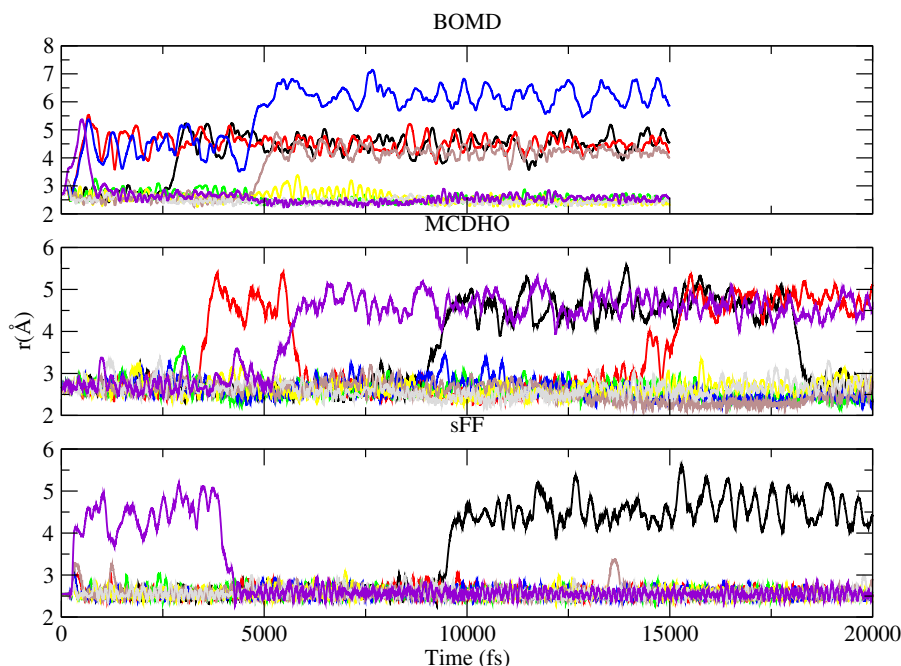


Figure S21: Pb-O distances found in the simulations of the 8+0 cluster (see fig. 1 of main text) by means of: BOMD simulation (top), classical MD with MCDHO (middle) and classical MD with the sFF of de Araujo et al.⁸ (bottom). Only the first 20 ps are shown.

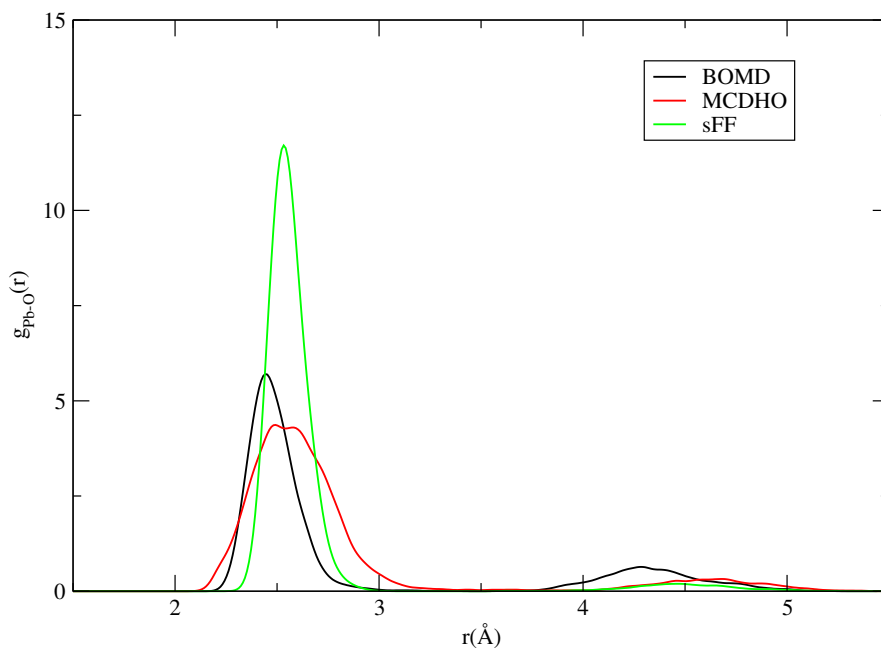


Figure S22: RDF's of the simulations of the 8+0 cluster (see fig. 3 of main text) employing: BOMD simulation, classical MD with MCDHO and classical MD with the sFF of de Araujo et al.⁸

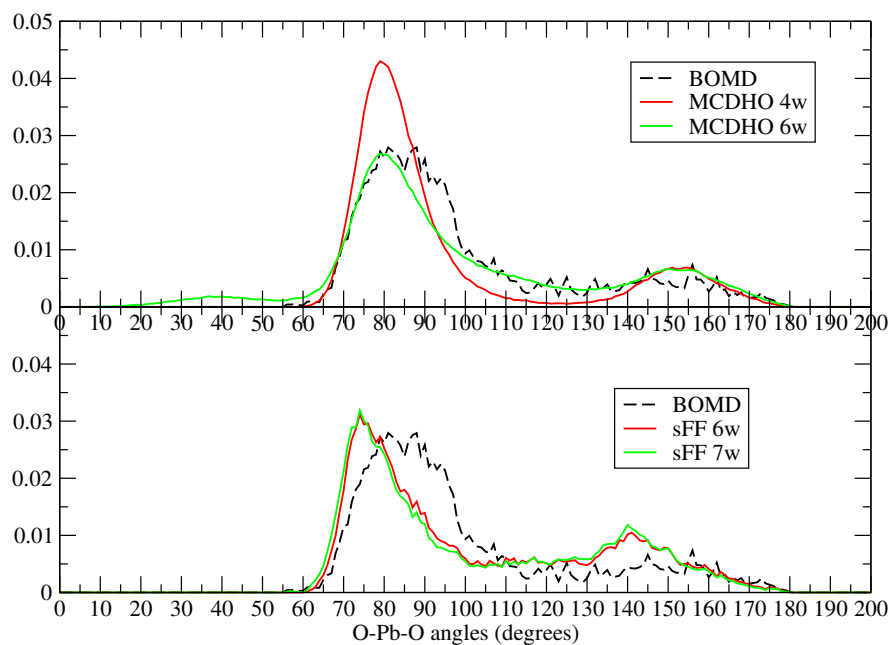


Figure S23: ADF's of the simulations of the 8+0 cluster (see fig. 1 of main text) employing: BOMD simulation, classical MD with MCDHO and classical MD with the sFF of de Araujo et al.⁸

References

- (1) Villa, A.; Hess, B.; Saint-Martin, H. Dynamics and Structure of Ln(III)-Aqua Ions: A Comparative Molecular Dynamics Study Using ab Initio Based Flexible and Polarizable Model Potentials. *J. Phys. Chem. B* **2009**, *113*, 7270–7281.
- (2) Darden, T.; York, D.; Pedersen, L. Particle Mesh Ewald: An $N \cdot \log(N)$ Method for Ewald Sums in Large Systems. *J. Chem. Phys.* **1993**, *98*, 10089–10092.
- (3) Essmann, U.; Perera, L.; Berkowitz, M. L.; Darden, T.; Lee, H.; Pedersen, L. G. A Smooth Particle Mesh Ewald Method. *J. Chem. Phys.* **1995**, *103*, 8577–8593.
- (4) Saint-Martin, H.; Hernández-Cobos, J.; Bernal-Uruchurtu, M. I.; Ortega-Blake, I.; Berendsen, H. J. C. A Mobile Charge Densities in Harmonic Oscillators (MCDHO) Molecular Model for Numerical Simulations: The Water–Water Interaction. *J. Chem. Phys.* **2000**, *113*, 10899–10912.
- (5) Mas, E. M.; Bukowski, R.; Szalewicz, K. Ab Initio Three-Body Interactions for Water. II. Effects on Structure and Energetics of Liquid. *J. Chem. Phys.* **2003**, *118*, 4404–4413.
- (6) Persson, I.; Lyczko, K.; Lundberg, D.; Eriksson, L.; Płaczek, A. Coordination Chemistry Study of Hydrated and Solvated Lead(II) Ions in Solution and Solid State. *Inorg. Chem.* **2011**, *50*, 1058–1072.
- (7) Etschmann, B. E.; Mei, Y.; Liu, W.; Sherman, D.; Testemale, D.; Müller, H.; Rae, N.; Kappen, P.; Brugger, J. The Role of Pb(II) Complexes in Hydrothermal Mass Transfer: An X-ray Absorption Spectroscopic Study. *Chem. Geol.* **2018**, *502*, 88–106.
- (8) de Araujo, A. S.; Sonoda, M. T.; Piro, O. E.; Castellano, E. E. Development of New Cd^{2+} and Pb^{2+} Lennard-Jones Parameters for Liquid Simulations. *J. Phys. Chem. B* **2007**, *111*, 2219–2224.

- (9) Hess, B.; Kutzner, C.; van der Spoel, D.; Lindahl, E. GROMACS 4: Algorithms for Highly Efficient, Load-Balanced, and Scalable Molecular Simulation.
- (10) León-Pimentel, C. I.; Amaro-Estrada, J. I.; Hernández-Cobos, J.; Saint-Martin, H.; Ramírez-Solís, A. Aqueous Solvation of Mg(ii) and Ca(ii): A Born-Oppenheimer Molecular Dynamics Study of Microhydrated Gas Phase Clusters. *J. Chem. Phys.* **2018**, *148*, 144307.